Clays and Clay Minerals, Vol. 39, No. 2, 191–201, 1991.

EVOLUTION OF THE POROUS STRUCTURE AND SURFACE AREA OF PALYGORSKITE UNDER VACUUM THERMAL TREATMENT

J. M. CASES,[1] Y. GRILLET,[2] M. FRANÇOIS,[1] L. MICHOT,[1]
F. VILLIÉRAS,[1] AND J. YVON[1]

[1] Centre de Recherche sur la Valorisation des Minerais et U.A. 235- B.P. 40
54501 Vandœuvre Cédex, France

[2] Centre de Thermochimie et de Microcalorimétrie - 26, rue du 141ème R.I.A.
13003 Marseille, France

Abstract—The modification of the external surface area and the two types of microporosity of palygorskite (structural and interfiber porosity) were examined as a function of the temperature of a vacuum thermal treatment to 500°C. The methods used included: controlled-transformation-rate thermal analysis, N_2 and Ar low-temperature adsorption microcalorimetry, conventional and continuous gas-adsorption volumetry (for N_2 and Ar) at 77 K and CO_2 at 273 and 293 K, water vapor adsorption gravimetry, and immersion microcalorimetry in water. At temperatures <100°C only 18% of the structural microporosity was available to N_2, 13% to Ar, and 100% to CO_2 at 273 K. In both experiments the channels filled at very low relative pressures. At temperatures between 70° and 130°C the structure folded, and the mineral transformed to anhydrous palygorskite, which showed no structural microporosity. The interfiber microporosity was found to be independent of the temperature treatment, and the external surface area decreased slightly from 65 to 54 m^2/g. The water adsorption isotherms showed that the folding of the structure was reversible up to final outgassing temperatures >225°C.

Key Words—Adsorption, Microcalorimetry, Microporosity, Palygorskite, Surface area, Thermal treatment.

INTRODUCTION

Palygorskite and sepiolite belong to a family of hydrous silicate minerals, rare in nature, but used by man for centuries because of their many diverse and useful sorptive properties. For example, Nederbragt and de Jong (1946) and Nederbragt (1949) described the adsorption on palygorskite of n-paraffins dissolved in pentane and of analogous branch-chain paraffins. They reported a selectivity in the adsorption of n-paraffins on the mineral. Several investigations have been undertaken, under systematically altered conditions of outgassing, to determine whether, and how readily, intracrystalline sorption by palygorskite occurs (Barrer and Mackenzie, 1954; Barrer *et al.*, 1959). These authors concluded that water and ammonia could diffuse into the channels after appropriate initial outgassing, with much less penetration by simple alcohols. Sorption of most species, including nitrogen and other nonpolar molecules, has been reported to be confined to corrugated external surfaces of the fibers or to sites just at the channel entrances. In fact, the sorption has been found to be substantial because of the extremely fine fibrous nature of the crystal and its correspondingly large external area (Fernandez Alvarez, 1978).

The structure of palygorskite can be regarded as consisting of ribbons of 2:1 phyllosilicate structure, one ribbon being linked to the next by inversion of SiO_4 tetrahedra along a set of Si–O–Si bonds. The ribbons are parallel to the X axis of the structure and have an average width along Y equivalent to two linked pyroxene-like single chains. The linked ribbons, thus, form a 2:1 layer continuous along X, but of limited lateral extent along Y. The average half unit-cell parameters of palygorskite are: a = 5.2 Å, b = 17.9 Å, $c \sin\beta$ = 12.7 Å (Bradley, 1940; Drits and Sokolova, 1971). Channels in the structure exhibit internal pores 3.7 Å × 6.4 Å in size, which are parallel to the fiber length. In the channel two water molecules are coordinated to each magnesium ion at the edges of structural ribbons. For a half unit cell, four H_2O molecules are bound to each octahedral cation, and four others are present as zeolitic water. On heating, the bound water molecules are lost in two stages: after the first two water molecules are lost, the structure collapses by alternate rotation of ribbons (Serna *et al.*, 1974, 1975; Rautureau and Tchoubar, 1976; Rautureau *et al.*, 1979; Van Scoyoc *et al.*, 1979), followed by a decrease in surface accessible to N_2 (Fernandez Alvarez, 1978; Jones and Galan, 1988). Palygorskite shows a nearly cylindrical habit. Generally, individual fibers are separated substantially from one another, and typically the fibers form bundles with frayed ends. The association of fibers produces an interfiber microporosity (Grillet *et al.*, 1988). The external surface consists predominantly of {011} crystal corrugated faces (Fenoll Hach-Ali and Martin Vivaldi, 1968; Martin Vivaldi and Fenoll Hach-Ali, 1969). Theoretical average external and internal surfaces have been estimated as 300 m^2/g external and 600 m^2/g internal for palygorskite from Attapulgus, Georgia (Serna and Van Scoyoc, 1979). In palygorskite, the surface area available depends mainly on the nature of

the molecules (size, shape, polarity) used as an adsorbate to penetrate the intra- or structural microporosity, the pretreatment (temperature and extent of outgassing), and the method used for adsorption (Grillet *et al.*, 1988; Michot *et al.*, 1990).

Most studies have been based on adsorption isotherms obtained from conventional volumetric adsorption apparatus, typically using N_2. Such techniques, however, are unable to reveal information at relative pressures <0.07. Hence, the usual method to detect and study microporosity (Lippens and de Boer, 1965; Sing, 1967; Sing *et al.*, 1985) cannot be used to reveal various types of microporosity (Dubinin, 1966) of palygorskite.

The present study of the microporous structure of palygorskite is based on the well-controlled thermal treatment and outgassing procedures used to study sepiolite (Grillet *et al.*, 1988), i.e., nitrogen or argon adsorption microcalorimetry (at 77 K), a continuous volumetric procedure for gas adsorption, which yields information in the low pressure range; and immersion microcalorimetry in water, which allows surface area to be determined by the so-called "absolute" method of Harkins and Jura (1944).

EXPERIMENTAL

Materials

The palygorskite studied here was from the Montagne de Reims, France, and was supplied by B.R.G.M. (Orléans, France). The approximate structural formula has been calculated according to a method recently proposed by Yvon *et al.* (1990) that takes into account of bulk chemical analysis, X-ray powder diffraction data, and electron microprobe analysis. The calculations, based on the model of Drits and Sokolova (1971) led to the formula: $Si_8(Al_{1.38}Fe^{3+}_{0.22}\ Fe^{2+}_{0.31}\square 0.89)O_{20}(OH)_2(H_2O)_4(H_2O)_4K_{0.13}Na_{0.01}Ca_{0.02}$, where $\square$ symbolizes a vacant site. The mineralogical purity of this sample was >93%. The major impurities were quartz (4%), anorthite (0.8%), calcite (0.6%), anatase (0.5%) and mica (1%).

Under the transmission electron microscope, fibers ranged in size from 0.5 to 2 μm in length, and 250 to 360 Å in width.

Controlled transformation-rate thermal analysis (CTRTA)

The method was described under the name of "reciprocal thermal analysis" by Grillet *et al.*, 1988 and Rouquerol (1970, 1989). In conventional thermal analysis, a physical property of a substance is measured as a function of temperature. The substance is subjected to a controlled temperature program, which is nearly always linear with time. For clay minerals, this type of procedure usually results in a partial overlap of successive dehydration or outgassing steps. In the present study, this problem was overcome by applying controlled transformation-rate thermal analysis (Rouquerol, 1970, 1989). In this process, the rate of dehydration or outgassing is kept constant (or controlled) over the entire temperature range of the experiment by means of an appropriate heating control loop, which results in an *a priori* unknown temperature program. The system operates in the reverse way of conventional thermal analysis, because the temperature is measured while a temperature-dependent property of the substance (here, the water content) is modified at a constant (or controlled) rate. In CTRTA, the rate of dehydration of the clay may be controlled at any value low enough to ensure a satisfactory elimination of the temperature and pressure gradients within the sample, i.e., to ensure a satisfactory separation of the successive steps of the dehydration. This simplest assembly is that of Rouquerol (1970), in which the flow of gas evolved from the sample submitted to a dynamic vacuum is used to control the heating of the furnace. For a constant composition of the gas evolved (here, water vapor), the temperature-vs.-time data may be immediately converted into temperature-vs.-mass-loss-data (inasmuch as the rate of dehydration is constant), and therefore to a conventional thermogravimetric curve. The experimental conditions selected in the present study were: a sample mass of 250–270 mg, a residual pressure of 2 Pa over the sample, and a dehydration rate of 2.77 mg/hr.

Gas adsorption microcalorimetry at 77 K

Gas-adsorption microcalorimetry (Rouquerol, 1972; Grillet *et al.*, 1988) allows a simultaneous recording of the adsorption isotherm of nitrogen or argon and the corresponding derivative enthalpy. For that purpose, the adsorbable gas is introduced into the adsorption cell at a slow and constant flow rate, under quasi-equilibrium conditions. The adsorption cell is surrounded by an isothermal microcalorimeter kept at 77 K by total immersion in a liquid nitrogen bath. Both the quasi-equilibrium pressure (by means of a diaphragm pressure transducer) and the heat flow, due to the adsorption phenomenon, may then be recorded as a function of time. A computer program derives the adsorption isotherm, the content of a monolayer (as calculated from the BET equation), and the derivative (or differential) enthalpy of adsorption vs. coverage (the latter being taken equal to 1, for the completion of the monolayer). In the present study, prior to each experiment 300–400-mg samples were outgassed, under the CTRTA conditions given above, to final temperatures of 25°, 100°, 130°, 150°, 225°, 380° and 500°C.

Adsorption gravimetry of water vapor

The experimental apparatus (Poirier *et al.*, 1987) derived from the apparatus described by Rouquerol and Davy (1978). It was built around a Setaram MTB

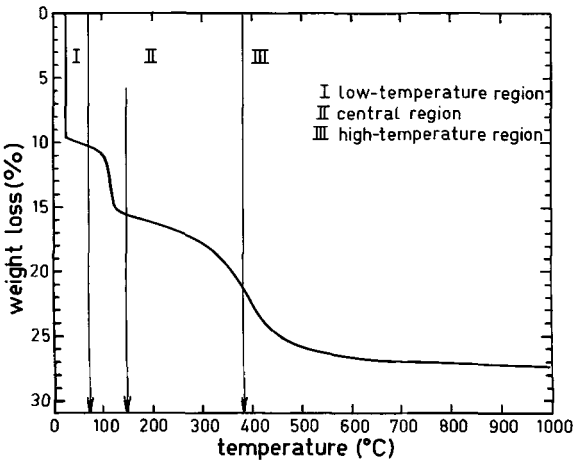

Figure 1. Controlled transformation rate thermal analysis of Montagne de Reims palygorskite.

10-8 symmetrical microbalance. Prior to each experiment, 100-mg samples were outgassed at a residual pressure of 0.1 Pa for 18 hr and at temperatures of 25°, 70°, 100°, 130°, 225°, 300°, 380°, and 500°C. Water vapor was supplied from a source kept at 41°C, here again at a slow flow-rate (through a Granville-Philips leak valve) to ensure quasi-equilibrium conditions at all times. The adsorption isotherm (i.e., mass adsorbed at 303 K vs. quasi-equilibrium pressure) was directly recorded on a simple X-Y recorder.

Immersion microcalorimetry in water

Immersion microcalorimetry was used to determine the enthalpy of immersion in water of the palygorskite sample vs. the pre-equilibration P/P_0 relative pressure of water vapor. The enthalpy curve was then used to derive the external (i.e., non-microporous) surface area by applying a modified Harkins and Jura method (Partyka *et al.*, 1979; Cases and François, 1982; Fripiat *et al.*, 1982). Details of the method were described by Grillet *et al.*, (1988). In the present study a sample mass of about 0.4 g was used, and the sample was outgassed at 25°C under the conditions given above for adsorption gravimetry of water vapor.

Nitrogen, argon, and CO_2 adsorption volumetry

Complete nitrogen adsorption-desorption cycles were determined using a conventional BET volumetric equipment (Delon, 1970). Prior to each experiment, 0.5 g of sample was outgassed at a residual pressure of 0.1 Pa for 18 hr and temperature of 25°, 100°, 130°, 225°, 300°, and 380°C.

The quasi-equilibrium gas adsorption procedure reported by Michot *et al.* (1990) was used to examine surface heterogeneity and microporosity of palygorskite in more detail. With this method a slow, constant and continuous flow of adsorbate (here, nitrogen and argon at 77 K, CO_2 at 273 and 293 K) was introduced into the adsorption cell. From the recording of the quasi-equilibrium pressures ($0.01–5 \times 10^4$ Pa) vs. time, the adsorption isotherms were derived. The experimental conditions were a sample mass of about 0.4 g, outgassing at 0.1 Pa to final temperatures of 25°, 70°, 130°, 150°, 225°, 300°, and 380°C for N_2 and Ar.

RESULTS

Figure 1 shows the controlled transformation-rate thermal analysis curve for the palygorskite sample. The curve can be divided into three parts: (I) a low-temperature region; (II) a central region and (III) a high-temperature region. In the low-temperature region (<75°C), the curve shows a sharp decrease at 25°C (weight loss = 8.95% of the final mass) followed by a gradual decrease to 75°C, the point of inflexion of the first subplateau. This region corresponds mainly to the loss (10.17% of the final mass) of zeolitic and adsorbed water on external surfaces (Table 1). In the central region (75°–370°C), the total weight loss is 10.48% of the final mass due to loss of coordination water. According to Serna *et al.* (1975), the crystal folds if about half the water of hydration (i.e., water coordinated at the edge Mg atoms inside the channels) is removed. In these conditions, under vacuum, the region between 75° and 150°C (weight loss = 5.24%) corresponds main-

Table 1. Theoretical and observed water losses (wt.%) for palygorskite.

	Low-temperature region	Central region		High-temperature region	Total weight losses
Temperature range (°C)	25–72	72–370		>370	—
		72–150	150–370		
Theoretical weight losses from structural formula (wt.%)	10.48	5.24	5.24	2.62	23.58
	Zeolitic water	Bound water		Structural water	
Practical weight losses (wt.%)	10.17	5.24	5.24	6.62	27.27
	Zeolitic and adsorbed water	Bound water		Structural and trapped water, decarbonation	—

https://doi.org/10.1346/CCMN.1991.0390211 Published online by Cambridge University Press

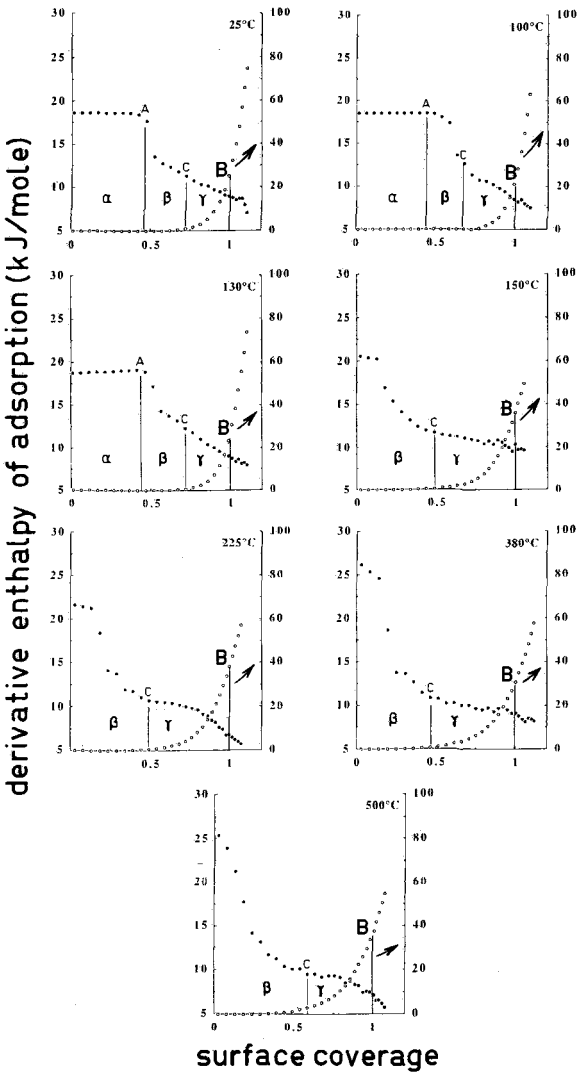

Figure 2. Derivative enthalpy of adsorption (solid circle) and equilibrium pressure (open circle) vs. coverage for palygorskite-nitrogen system at 77 K.

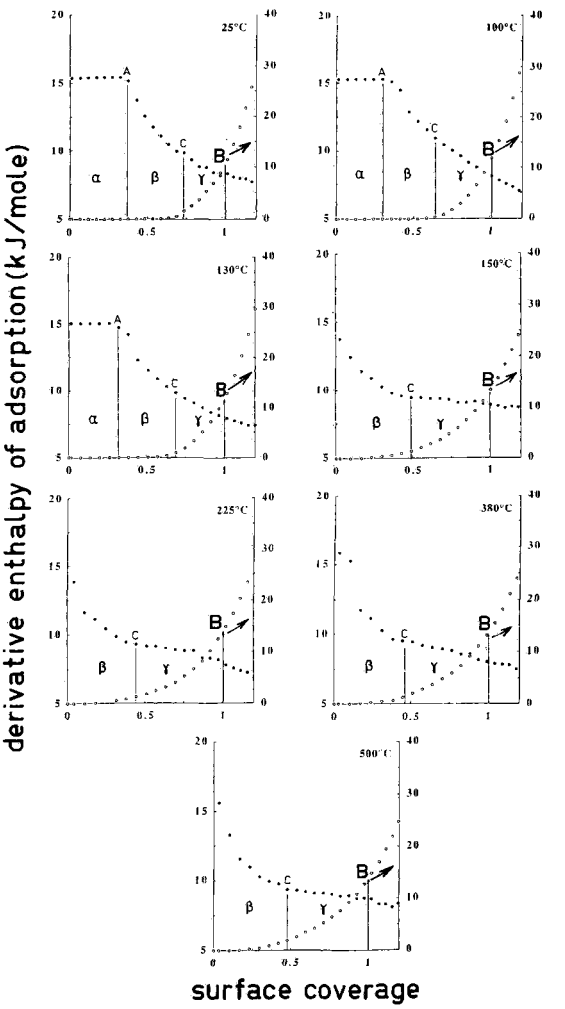

Figure 3. Derivative enthalpy of adsorption (solid circle) and equilibrium pressure (open circle) vs. coverage for palygorskite-argon system at 77 K.

ly to the folding of the structure, i.e., the removing of two of the four coordinated water molecules per half-cell. In the high-temperature region (>370°C) the weight loss represents dehydroxylation of the structure (2.61% of the final mass), the removal of the remaining water in collapsed channels (3.70% of the final mass), and decomposition of calcite (0.30%). The difference between the total weight loss and the theoretical weight loss calculated from the approximate structural formula (3.39%) can be mainly attributed to adsorbed water on external surfaces of the initial sample.

In vacuum, the observed temperature ranges were lower than those observed under atmospheric pressure (Jones and Galan, 1988). Except for the first two water molecules bound to Mg, however, the assignement of the water percentage calculated from the CTRTA curve to the different types of water is more difficult here than for sepiolite (Grillet *et al.*, 1988).

Shown in Figure 2 are derivative enthalpies of nitrogen vs. coverage, at 77 K, for a series of seven samples outgassed to different extents, along with corresponding adsorption isotherms. Coverage, defined as the ratio between the adsorbed quantity to the monolayer capacity, was calculated by assuming it to be unity at point B of the adsorption isotherm (Emmet and Brunauer, 1937). This point was close to, but always slightly less than, the point at which the enthalpy of adsorption merges into the enthalpy of liquefaction. These complex enthalpy curves could not be obtained by the isosteric method, which lacks accuracy in the low-pressure range, if adsorption isotherms were determined from conventional adsorption volumetric apparatus (Figure 4). A similar set of curves obtained for argon also at 77 K is given in Figure 3.

Adsorption-desorption isotherms obtained with ni-

https://doi.org/10.1346/CCMN.1991.0390211 Published online by Cambridge University Press

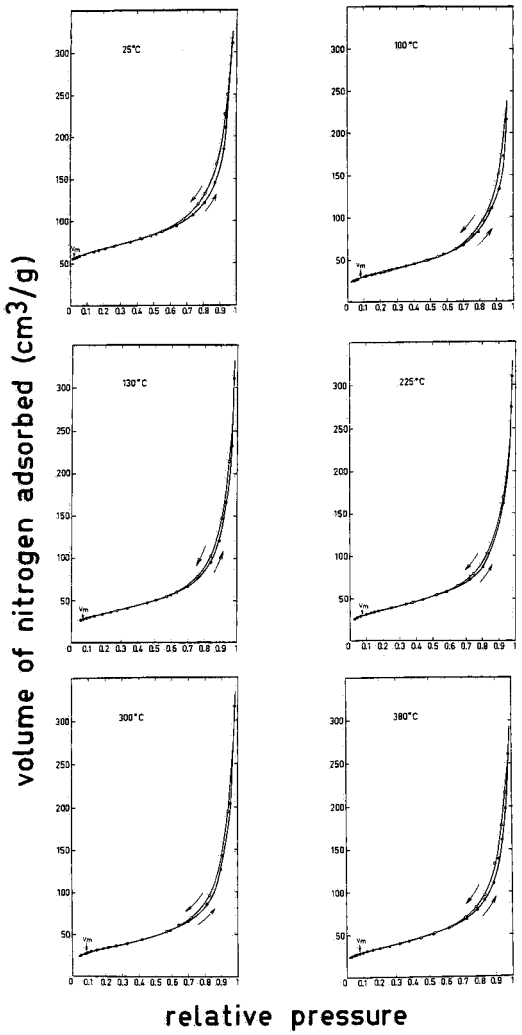

Figure 4. Adsorption-desorption isotherms of nitrogen at 77 K for palygorskite obtained from conventional adsorption volumetric equipment.

trogen, using a conventional volumetric apparatus, are given in Figure 4. These isotherms have the characteristic feature of the type IV isotherm, with very limited hysteresis loops, which were probably due to capillary condensation in mesopores. This behavior is characteristic of low degree of mesoporosity. The adsorption isotherms given in Figure 4 were replotted following the procedure of de Boer *et al.* (1966) in the form Va vs. t, where t is the mean thickness of the adsorbed layer (which is known from a reference curve obtained using the same adsorbate, but with a nonmicroporous adsorbent); and Va the total amount of adsorbate in the adsorbed layer, expressed as volume at s.t.p. In this plot, an upward deviation commencing above point B indicates the inception of capillary condensation. The original slope of the t-plot indicates the total surface area, whereas a positive intercept i (converted to liquid volume) indicates the presence of micropores having a total volume equivalent to i. The corresponding slope of this new straight line allowed the remaining surface area to be determined (outer surface and/or surface in wide pores), as noted in Table 2 (the column labeled S_{ext}). The t-curve was, if possible, chosen to have the same value of the energetic constant C as the system under consideration (Mikhail *et al.*, 1968).

Table 2. Equivalent specific surface area (m^2/g) obtained with nitrogen conventional volumetric apparatus.

Final outgassing temperature (°C)	BET parameters			t plot		
	V_m liq (cm^3/g) 1	S (m^2/g) 2	C 3	S_{total} (m^2/g) 4	V_0 liq (cm^3/g) 5	S_{ext} (m^2/g) 6
25	0.0871	247	1129		0.0500	125
100	0.0445	126	132	124	0.0038	114
130	0.0440	125	132	126	0.0062	111
225	0.0462	131	184		0.0069	116
300	0.0429	122	121	122	0.0062	103
380	0.0437	124	139	125	0.0074	107

(1) Monolayer capacity calculated from the BET equation per unit mass of adsorbent as calculated with the density of the liquid adsorptive; (2), (4) total specific surface area; (3) energetic constant of BET theory; (5) micropore volume per unit of adsorbent as calculated with the density of the liquid adsorptive; (6) external specific surface area.

Adsorption isotherms obtained by the quasi-equilibrium gas adsorption procedure allowed surface heterogeneity to be examined in the low-pressure range. Results are given in Figure 5 for nitrogen and in Figure 6 for argon as surface coverage vs. undersaturation (Cases, 1979). The undersaturation is the napierian logarithm of the relative pressure P/P_0, P is the equilibrium pressure and P_0 the saturation pressure of the pure adsorbate at the temperature of the measurement. The equivalent specific surface areas calculated from the BET equation are given in Table 3.

The quasi-equilibrium gas adsorption procedure using CO_2 at 273 and 293 K was used to study changes in microporosity during outgassing. Dubinin's equation (1966) was applied:

$$\log V = \log V_0 - D[\log[P_0/P]]^2$$

where V is the volume of gas adsorbed, V_0 is the volume of gas (cm^3/g), which, once adsorbed, is able to completely fill micropores, and P_0 the saturating vapor pressure. V_0 was converted into liquid volume V_0 (liq) using densities of 1.08 and 1.05 g/cm^3 for liquid CO_2 at 273 and 293 K, respectively (Anonymous, 1976). The results are presented in Table 4.

The adsorption-desorption isotherms of water at 303 K at the different outgassing temperatures are given in Figure 7. The location of the monolayer, as calculated by the BET method, is indicated on each isotherm by Q_m. The exact value of V_m, the liquid volume (cm^3/g) of water corresponding to the monolayer capacity, is

https://doi.org/10.1346/CCMN.1991.0390211 Published online by Cambridge University Press

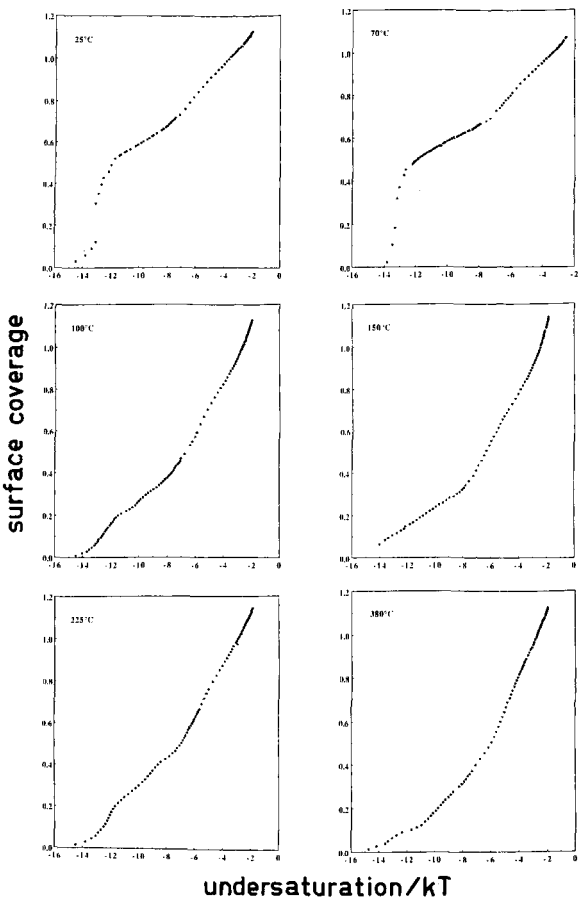

Figure 5. Adsorption isotherms of nitrogen at 77 K for palygorskite obtained from quasi-equilibrium gas adsorption procedure.

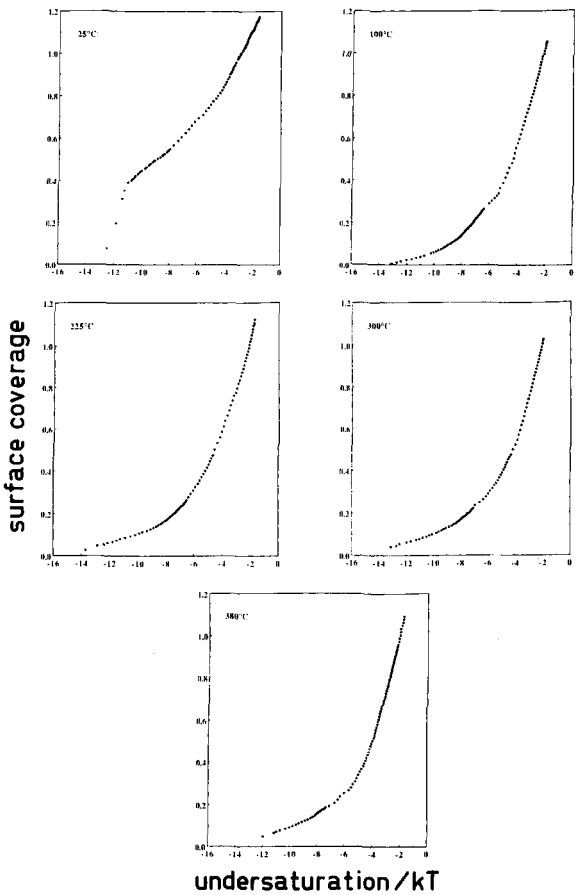

Figure 6. Adsorption isotherms of argon at 77 K for palygorskite obtained from quasi-equilibrium gas adsorption procedure.

given in Table 5, column 3. The corresponding value of the BET energetic constant C (column 5) and the equivalent specific surface area calculated with a molecular area of 14.8 Å² (Hagymassy *et al.*, 1969) are also given (column 4 and Figure 8).

The enthalpy of immersion of palygorskite in saturated solution, after outgassing and increasing precoverage relative pressures, decreased from 91.2 J/g for the immersion of the bare solid to an approximately constant value of 7.5 J/g for precoverage relative pressure >0.75. This value was used to derive the external specific surface area, following the Harkins and Jura method, using a value of 119 mJ/m² for the internal energy of the water surface at 303 K (Cases and François, 1982). The result was 63 m²/g for the sample outgassed at a final temperature of 25°C.

Table 3. Equivalent specific surface areas obtained with nitrogen and argon from quasi-equilibrium gas adsorption procedure.

Final outgassing temperature (°C)	Nitrogen			Argon			
	V_m liq (cm^3/g)	S (m^2/g)	C	V_m liq (cm^3/g)	S (m^2/g)	C	$\frac{(V_B)\ Ar}{(V_B)\ N_2}$
	1	2	3	5	6	7	
25	0.0845	240	1300	0.0664	197	306	0.786
70	0.0884	251	936				
100	0.0445	126	177	0.0360	107	58	0.808
150	0.0464	132	109				
225	0.0414	118	306	0.0372	112	55	0.898
300				0.0364	108	48	
380	0.0428	122	202	0.0370	110	48	0.864

(1), (5) Monolayer capacity calculated from the BET equation per unit mass of adsorbent as calculated with the density of the liquid adsorptive; (2), (6) total specific surface area; (3), (7) energetic constant of BET theory.

https://doi.org/10.1346/CCMN.1991.0390211 Published online by Cambridge University Press

Table 4. Micropore volumes V_0 (liq : cm^3/g) of palygorskite obtained from CO_2 adsorption.

Adsorption temperature (K)	Final outgassing temperature (°C)				
	25	70	100	130	150
273	0.2279	0.2556	0.1438	0.0241	
293	0.2274		0.0719		0.0373

INTERPRETATION OF THE ADSORPTION ENTHALPY DATA

As previously described for sepiolite (Grillet *et al.*, 1988), three distinct ranges of relative pressure may be identifed for samples outgassed at ≤130°C. These are denoted by α, β, and γ in Figures 2a (nitrogen adsorption) and 3a (argon adsorption).

Range α extends to point A on the curves. For this range, the derivative enthalpy of adsorption was constant with adsorption. The same has been observed for adsorption on homogeneous surfaces, such as molecular sieves. This range appears to correspond to the filling of structural micropores. The α domain disappeared if the sample was outgassed at >130°C due to the folding of the structure if about half of the bound water was driven off (Figure 1, Table 1).

Range β lies between points A and C; here the derivative enthalpy decreased with coverage. Commonly, point C is an inflection point or a point at which the slope changes. The point C is often the point at which the straight line extrapolated from the straight line of range γ leaves the experimental curve. By analogy with sepiolite (Grillet *et al.*, 1988), range β probably corresponds to the filling of wider micropores than those filled in range α, although this range (β) existed at very low pressures. As seen in Figures 2 and 3, point C was always reached for relative pressures <0.01, except for the system argon-palygorskite outgassed at 25°C (relative pressure 0.035). These latter micropores may represent either inter fiber microporosity or, more probably, defects in the arrangement of structural units (Rautureau and Tchoubar, 1976). The wide range of derivative enthalpies suggests a wide range in micropore size. This type of micropore will be referred to as interfiber microporosity.

Finally, the external surface areas were derived as for sepiolite (Grillet *et al.*, 1988) from the amount adsorbed over range γ (to point B) (cf. Table 6, columns 6 and 10), in which the surface coverage increase corresponds to an appreciable increase of the equilibrium pressure.

The amount of either nitrogen or argon corresponding to the filling in range α and β may be converted into liquid volume using the values of 0.808 and 1.427 (Anonymous, 1976) for the specific gravity of liquid nitrogen and liquid argon, respectively (Table 6, columns 5 and 9). The liquid volume V_B corresponding

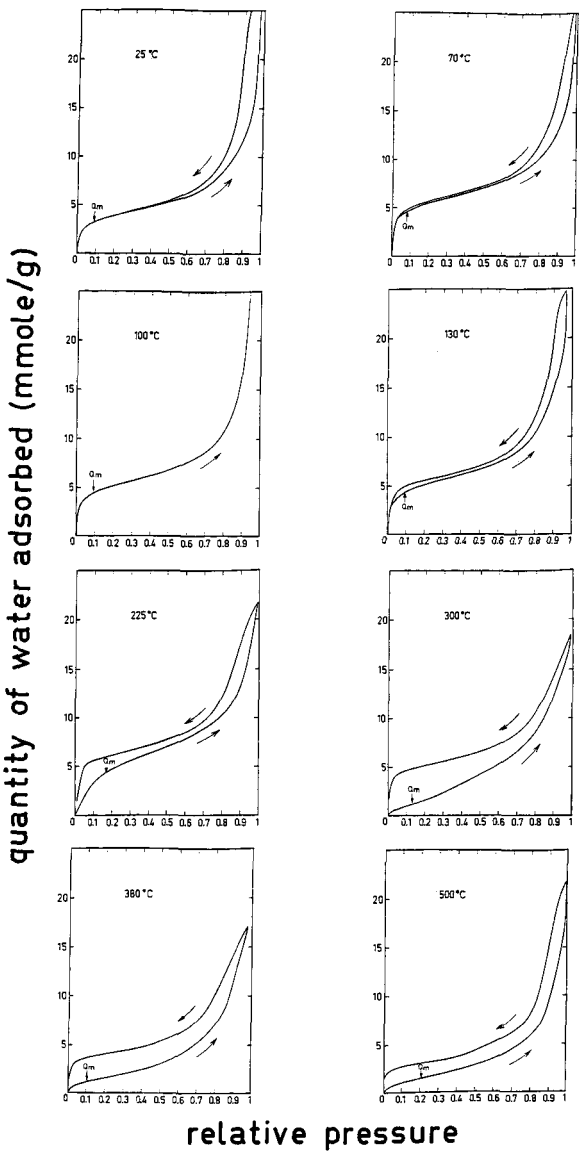

Figure 7. Influence of outgassing temperature on adsorption isotherms of water for palygorskite at 303 K.

to the monolayer capacity, i.e., the amount adsorbed at "point B" (Emmett and Brunauer, 1937), may also be calculated, and a specific surface area "S_{total}" may be derived, assuming cross sectional areas of 16.2 and 13.8 Å^2 for the nitrogen and argon molecules, respectively (McClellan and Harnsberger, 1967) (Table 6, columns 3, 4, 7, and 8). The word "equivalent" is included to emphasize the partial inadequacy of the above calculation for a microporous solid in which the adsorbed molecules do not cover at all the same area as on a flat surface (Sing *et al.*, 1985). Finally, the amount adsorbed in range γ to point B yields information on the external surface area of the corrugated fibers S_{ext} (Table 6, columns 6 and 10). To confirm the

https://doi.org/10.1346/CCMN.1991.0390211 Published online by Cambridge University Press

Table 5. Equivalent specific surface area and energetic constant as calculated from the BET theory and obtained from water adsorption.

Final outgassing temperature (°C)	Q_m (mmole/g) (1)	V_m (cm^3/g) (2)	S_{total} (m^2/g) (3)	C (4)
25	3.32	0.0580	287	114
70	4.55	0.0819	406	156
100	4.47	0.0805	399	109
130	4.30	0.0774	381	96
225	4.47	0.0819	399	22.5
300	1.10	0.0198	98	25
380	1.10	0.0198	98	50
500	1.15	0.0270	135	13

(1) Monolayer capacity amount; (2) monolayer capacity liquid volume calculated from the BET equation per unit mass of adsorbent; (3) total specific surface area; (4) energetic constant of BET theory.

hypothesis on the physical meaning of the three ranges, a series of complementary studies was undertaken.

Determination of the external area of fibers

For the sample outgassed at 25°C, the external area of fiber was determined by three procedures. The first used the Harkins and Jura procedure and the plot of enthalpy of immersion vs. relative pressure of water precoverage (Grillet *et al.*, 1988). The result was 63 m^2/g. The second procedure made use of the statistical measurement by transmission electron microscopy. The

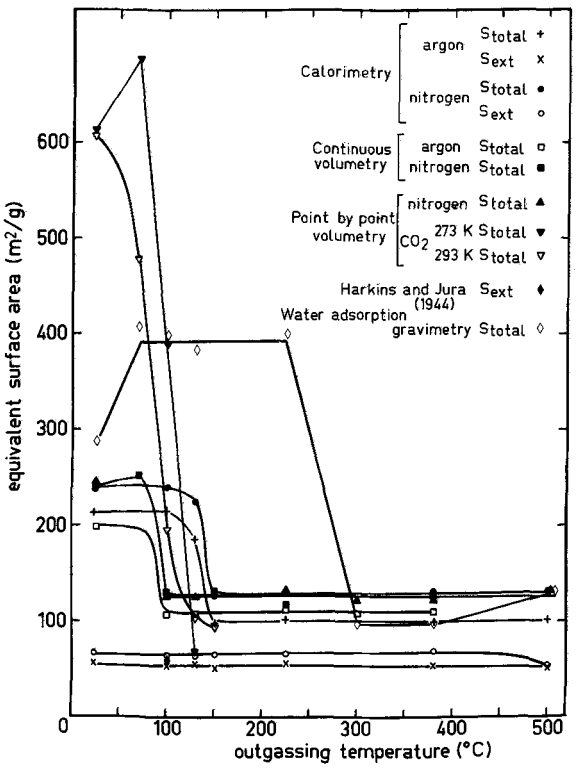

Figure 8. Effect of heat treatment on the equivalent specific surface area and external surface area of palygorskite obtained with different adsorbates and methods.

Table 6. Low-temperature adsorption calorimetry results for palygorskite.

Final outgassing temperature (°C)	N_2 adsorption at 77 K					Ar adsorption at 77 K				
	Range	S_{total} (m^2/g) (1)	V_B liq (cm^3/g) (2)	V_i (cm^3/g) (3)	S_{ext} (m^2/g) (4)	S_{total} (m^2/g)	V_B liq (cm^3/g)	V_i (cm^3/g)	S_{ext} (m^2/g)	$\frac{(V_B)\ Ar}{(V_B)\ N_2}$
25		238	0.0839		66.5	213	0.0718		56.7	0.856
	α			0.0388				0.0265		
	β			0.0217				0.0262		
	total			0.0605				0.0527		
100		238	0.0838		65.6	215	0.0724		54.2	0.864
	α			0.0369				0.0256		
	β			0.0238				0.0286		
	total			0.0607				0.0542		
130		223	0.0787		63.3	184	0.0619		57.1	0.786
	α			0.0347				0.0199		
	β			0.0217				0.0228		
	total			0.0564				0.0427		
150		126	0.0444		64.5	98.3	0.0331		50	0.746
	β			0.0216				0.0162		
225		130	0.0457		65.7	100.5	0.0339		56.1	0.741
	β			0.0226				0.0150		
380		132	0.0465		69.5	99	0.0334		53.4	0.718
	β			0.0220				0.0154		
500		132	0.0465		54.5	101	0.0342		53.3	0.735
	β			0.0273				0.0163		

(1) Total specific surface area; (2) monolayer capacity volume obtained from the B point per unit mass of adsorbent; (3) micropore volume per unit mass of adsorbent as calculated with density of the liquid adsorptive; (4) external specific surface area.

https://doi.org/10.1346/CCMN.1991.0390211 Published online by Cambridge University Press

fibers were found to range from 0.5 to 2.0 μm in length, and ~250 to ~360 Å in thickness. Assuming a square cross-section and taking into account a mean width of 300 Å and a specific gravity of 2.3 (Hénin and Caillère, 1975) leads to an external surface area of about 58 m^2/g. The third procedure made use of the value of the external surface area obtained from the amount adsorbed over range γ to point B (cf. Table 6, columns 6 and 10). The surface areas by this method were 66.5 and 56.7 m^2/g for nitrogen and argon, respectively. The arithmetical mean of all of the above values is about 60 m^2/g and may be taken as the external specific surface area of the palygorskite sample outgassed at 25°C. This value was apparently unaffected by the change in final outgassing temperature. The arithmetical mean obtained with nitrogen (64 m^2/g) was greater than for argon (54 m^2/g). The difference can be attributed to effective values of the cross sectional area of nitrogen and argon adsorbed on the surface. These values, as assumed for the calculation of the specifc surface area, are only valid for flat surfaces without roughness, i.e., not for corrugated palygorskite surface.

In contrast with previous results presented for sepiolite (Grillet *et al.*, 1988), no sintering was observed with vacuum thermal treatment.

Evaluation of structural microporosity

From Figures 1 and 8 and the results in Tables 2–6, the sharp diminution of weight by the loss of water observed on the CTRTA curve between 100° and 132°C, which corresponds to the expulsion of about half of the bound water and the folding of the structure, is clearly related to the decrease of the surface area. The equivalent surface area obtained with nitrogen ranged from 243 to 126 m^2/g and from 208 to 105 m^2/g with argon (arithmetical mean of all the volumes obtained). The BET or B point surface-area decrease was probably due to destruction of structural microporosity. The temperature of the first structural change (folding) was dependent on the pressure during outgassing and was between 70° and 100°C (Tables 2 and 3) and at about 130°–150°C (Table 6) for 0.1 and 2 Pa, respectively. For sepiolite, the decrease of equivalent surface area was found to be between 200° and 300°C, which is far from the weight loss due to bound water (150°C). Inasmuch as almost no water was evacuated between 200° and 300°C, these data suggest a progressive change in the structure of the fiber.

The microporous volume, calculated from the t-plot of de Boer *et al.* (1966), was found to be 0.0500 cm^3/g after outgassing at 25°C (Table 2), relatively close to that calculated from the adsorption enthalpy data. The microporous volume that corresponds to adsorption range α (0.0369 cm^3/g for nitrogen, 0.0260 cm^3/g for argon) was nil for the folded structure, considerably smaller than those calculated for CO_2 adsorption (~0.227 cm^3/g at 25°C and 0.2556 cm^3/g at 70°C) or from the theoretical dimension of the channels (0.2096 cm^3/g).

All these results show that the sorptive ability of palygorskite depended greatly on the outgassing pretreatment. Sorption of CO_2 was enhanced by the removal of water from channels by outgassing in vacuum at 70°C; this adsorbate completely filled the structural microporosity. Nitrogen was not able to penetrate into the channel structure easily, and argon was able to penetrate to an even lesser extent. Adsorption was, thus, predominantly in intermicroporosity and on external surfaces (Table 6). Only 17.6% and 12.6% of the structural microporosity were available for nitrogen and argon, respectively. These results may be explained by sizes calculated from the van der Waals sphere method of the CO_2 molecule (cylinder of 2.8 Å diameter and 5.12 Å length), N_2 molecule (cylinder of 3 Å diameter and 4 Å length), and Ar molecule (3.83 Å). The influence of the size was confirmed by results of the t-plot (Table 2); the calculated external surface area was close to the equivalent surface area for all the outgassing temperatures >100°C. These results are only dependent on the intermicroporosity and external surface area.

The sorption of water (Figure 8 and Table 5) was enhanced by the removal of water from channels by outgassing in vacuum to 225°C. The folding corresponding to the first structure change was reversible to the loss of the second part of the bound water. The decrease vs. surface area was in the same range of outgassing temperatures that has been reported for sepiolite (Grillet *et al.*, 1988).

Evaluation of interfiber microporosity

The corresponding volume (converted to equivalent liquid volume) was calculated from the adsorption range β (Figures 2 and 3, Table 6). It was probably due to inter-fiber micropores and structural defects. The volume of these micropores, always available to nitrogen (or CO_2), was found to be independent of the outgassing temperature (0.0223 cm^3/g between 25° and 380°C), but increased at 500°C, because of the formation of new structural defects due to dehydroxylation of the structure. Argon was unable to penetrate into all the interfiber microporosity. The values obtained (0.0163 cm^3/g) were lower than for nitrogen. In addition, the volume of these micropores available to argon decreased from 0.0228 to 0.0162 cm^3/g if the final outgassing temperature was increased from 130° to 150°C.

ENERGETIC CONSIDERATIONS

Along each abscissa in Figures 2 and 3, the difference in the derivative enthalpies between the nitrogen and argon allowed the determination of the specific interaction of the nitrogen molecules with the surface due to its quadrupole momentum: the values obtained were about −3.2 kJ/mole during the filling of range α, −0.7

https://doi.org/10.1346/CCMN.1991.0390211 Published online by Cambridge University Press

to −2.25 kJ/mole at point C, except for final outgassing temperature of 225° and 500°C, at which the differences were about 0.9 kJ/mole. The affinity of nitrogen for palygorskite was commonly greater than that of argon. Figures 2 and 3 show that an increase of the pretreatment temperature produced, for low surface coverages, an increase of the derivative enthalpies of nitrogen to 380°C, and then a decrease linked to the loss of the second part of the bound water, and a constant decrease for argon and outgassing temperature >100°C.

The nitrogen energetic constant of BET (Tables 2 and 3) decreased sharply from 25° to 150°C, reached a maximum at 225°C, and then decreased constantly to 380°C. For argon, a constant decrease was always observed (Table 2). The values calculated from the energetic constant are usually in good agreement with that observed on the derivative enthalpies in ranges β and γ, taking into account values of −6.7 and −5.6 kJ/mole for the enthalpies of liquefaction of nitrogen and argon respectively (Table 3).

The ratio (V_B) argon/(V_B) nitrogen (given in the last column of Tables 3 and 6) was always about 0.808, the ratio of the molar molecule of the two adsorbates obtained from the density in the liquid state. This ratio was also found in a fully microporous sample (Rouquerol *et al.*, 1984), meaning that nitrogen did not strongly interact with the surface or with the wall of the channel in range α.

In Figure 9, the water adsorption isotherms are plotted in the form θ (where $\theta = N_a/N_m$) vs. ln (P/P_0), where N_a represents the number of molecules adsorbed and N_m the monolayer capacity. Under any given conditions, the value of ln (P/P_0) at which the adsorption took place was directly related to the strength of the normal adsorbate-adsorbent interaction (Cases, 1979).

The displacement of the isotherms toward the high relative pressures suggests a loss of the normal interaction. The shape of the isotherms characterizes an important energetic heterogeneity. The affinity of water molecules for surface active sites increased slightly from 25° to 70°C, then decreased to 225°C, increasing again to 380°C, and then decreasing. The evolution was confirmed, in the same way, by the variation of the BET energetic constant C (Table 5, last column). For example, for a surface coverage value of 0.5, the gain of affinity for a mole can be estimated (Figure 9) to 1.1 RT between 225° and 380°C, and 0.8 RT from corresponding BET energetic constants. The variation observed in the range of the loss of the second part of the bound water (Figure 1) immediately before the dehydroxylation of palygorskite was probably due to a reversibility of this phenomenon in ranges β and γ.

SUMMARY AND CONCLUSIONS

From the present textural study of palygorskite from the Montagne de Reims the external surface area of the fiber was determined and two types of microporosity were detected. Interfibers or structural microporosity was fully available to CO_2 to about 0.21 cm^3/g and partly available to N_2 (17.6%), Ar (12.6%), and H_2O. The structural porosity completely disappeared by outgassing the sample at >130°C in the conditions of controlled transformation-rate thermal analysis and >70°C for smaller pretreatment pressures because of the folding of the structure. This phenomenon was partly reversible with water to 225°C, corresponding to the beginning of the loss of the second portion of the bound water. Sintering was not observed with increasing pretreatment temperature. Water adsorption isotherms revealed a maximum for the affinity of water for anhydrous palygorskite at about 380°C, suggesting that the loss of the second part of the bound water was a partly reversible phenomenon.

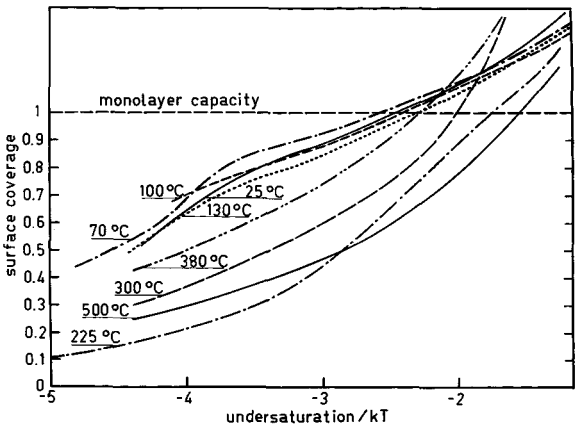

Figure 9. Adsorption isotherm for the palygorskite water systems at 303 K in the monolayer range and in the plane (θ, undersaturation /kT).

ACKNOWLEDGMENTS

This research was supported by the Phygis program of the French Ministry of Research. The authors are grateful to Michel Gres from B.R.G.M. (Orléans, France) which kindly supplied the sample of palygorskite.

REFERENCES

Anonymous (1976) *Gas Encyclopedia*: L'Air Liquide, ed., Elsevier, Amstedam, 1150 pp.

Barrer, R. M. and Mackenzie, N. (1954) Sorption by attapulgite. I. Availability of intracrystalline channels: *J. Phys. Chem.* **58,** 560–568.

Barrer, R. M., Mackenzie, N., and MacLeod, D. M. (1959) Sorption of attapulgite. II. Selectivity shown by attapulgite, sepiolite and montmorillonite for n-paraffins: *J. Phys. Chem.* **58,** 568–573.

Bradley, G. V. (1940) The structural scheme of attapulgite: *Amer. Mineral.* **25,** 405–410.

Cases, J. M. (1979) Adsorption des tensio-actifs à l'interface solide-liquide: Thermodynamique et influence de l'hétérogénéité des adsorbants: *Bull. Mineral.* **102,** 684–707.

Cases, J. M. and François, M. (1982) Etude des propriétés de l'eau au voisinage des interfaces: *Agronomie* **2,** 931–938.

de Boer, J. H., Lippens, B. C., Linsen, B. G., Broekhollf, J. C. P., Van den Heuvel, A., and Osinga, Th. J. (1966) The t-curve of multimolecular N_2 adsorption: *J. Colloid Interface Sci.* **21,** 405–414.

Delon, J. F. (1970) Contribution à l'étude de la surface spécifique et de la microporosité des minéraux et des roches: Thèse doctorat ès sciences physiques, Université de Nancy, Nancy, France, 187 pp.

Drits, V. A. and Sokolova, G. V. (1971) Structure of palygorskite: *Soviet Phys. Crystallogr.* **16,** 183–185.

Dubinin, M. M. (1966) Modern state of the theory of gas and vapor adsorption by microporous adsorbants: *Pure Appl. Chem.* **10,** 309–321.

Emmett, P. H. and Brunauer, J. (1937) The use of low temperature van der Waals adsorption isotherms in determining the surface area by ion synthetic ammonia catalyst: *J. Amer. Chem.* **59,** 1553–1564.

Fenoll Hach-Ali, P. and Martin Vivaldi, J. L. (1968) Contribution al estudio de la sepiolita: IV. Superficie especifica de los cristalles: *An R. Soc. Esp. Fis. Quim.* **64B,** 77–82.

Fernandez Alvarez, T. (1978) Effecto de la deshydratacion sobre las propriedades adsorbentes de la palygorskita y sepiolita. I. Adsorcion di nitrogeno: *Clay Miner.* **13,** 325–335.

Fripiat, J. J., Cases, J. M. François, M., and Letellier, M. (1982) Thermodynamic and microdynamic behavior of water in clay suspensions and gels: *J. Colloid Interface Sci.* **89,** 378–400.

Grillet, Y., Cases, J. M., François, M., Rouquerol, J., and Poirier, J. E. (1988) Modification of the porous structure and surface area of sepiolite under vacuum thermal treatment: *Clays & Clay Minerals.* **36,** 233–242.

Hagymassy, J., Brunauer, S., and Mikhail, R. Sh. (1969) Pore structure analysis by water vapor adsorption. I. t-curves for water vapor: *J. Coll. Interface Sci.* **29,** 485–491.

Harkins, W. D. and Jura, G. (1944) An absolute method for the determination of the area of a finely divided crystalline solid: *J. Amer. Chem. Soc.* **66,** 1362–1365.

Hénin, S. and Caillère, S. (1975) Fibrous minerals: in *Soil Components,* J. E. Gieseking, ed., Springer-Verlag, Berlin, 335–349.

Jones, B. F. and Galan, E. (1988) Sepiolite and palygorskite: in *Hydrous Phyllosilicates (Exclusive of Micas),* S. W. Bailey, ed., *Review in Mineralogy: Vol. 19,* Mineral. Soc. Amer., Washington, D.C., 628–674.

Lippens, B. C. and de Boer, J. H. (1965) Studies on pore systems in catalysis. V. The t-method: *J. Catalysis* **4,** 319–323.

McClellan, A. L. and Harnsberger, H. F. (1967) Cross sectional areas of molecules adsorbed on solid surfaces: *J. Colloid Interface Sci.* **23,** 577–599.

Martin Vivaldi, J. L. and Fenoll Hach-Ali, P. (1969) Palygorskite and sepiolite (hormites): in *Differential Thermal Analysis, Vol. 1, Fundamental Aspects,* R. C. Mackenzie, ed., Academic Press, London, 553–572.

Michot, L., François, M., and Cases, J. M. (1990) Continuous volumetric procedure for gas adsorption: A mean to study surface heterogeneity: *Langmuir* **6,** 677–681.

Mikhail, R. Sh., Brunauer, S., and Bodor, E. E. (1968) Investigation of a complete pore structure analysis. I. Analysis of micropores: *J. Colloid Interface Sci.* **26,** 43–53.

Nederbragt, G. W. (1949) Separation of long chain and compact molecules by adsorption on attapulgite containing clays: *Clay Min. Bull.* **3,** 72–75.

Nederbragt, G. W. and de Jong, J. J. (1946) The separation of long chain and compact molecules by adsorption: *Rec. Trav. Chim.* **65,** 831–834.

Partyka, S., Rouquerol, F., and Rouquerol, J. (1979) Calorimetric determination of surface areas. Possibilities of a modified Harkins and Jura procedure: *J. Colloid Interface Sci.* **68,** 21–31.

Poirier, J. E., François, M., Cases, J. M., and Rouquerol, F. (1987) Study of water adsorption on Na-montmorillonite. New data owing to the use of continuous procedure: in *Fundamentals of Adsorption,* T. Athanasios and T. Laiapis, eds., A.I.C.H.E., New York, 472–782.

Rautureau, M. and Tchoubar, C. (1976) Structural analysis of sepiolite by selected area electron diffraction. Relations with physicochemical properties: *Clays and Clay Minerals* **24,** 43–49.

Rautureau, M., Clinard, C., Mifsud, A., and Caillère, S. (1979) Etude microscopique de la palygorskite par microscopie électronique: in *Proc. 104ème Cong. Nat. des Sociétés Savantes* Bordeaux, Series Sciences, Vol. **3,** 199–212.

Rouquerol, J. (1970) L'analyse thermique à vitesse de décomposition constante: *J. Thermal Analysis* **2,** 123–140.

Rouquerol, J. (1972) *Calorimétrie d'Adsorption aux Basses Température. I. Thermochimie,* CNRS Publ., Paris, 538 pp.

Rouquerol, J. (1989) Controlled transformation rate thermal analysis: The hidden face of thermal analysis: *Thermodynamica Acta* **144,** 209–224.

Rouquerol, J. and Davy, L. (1978) Automatic gravimetric apparatus for recording adsorption isotherms of gases or vapours onto solids: *Thermodynamica Acta* **24,** 391–397.

Rouquerol, J., Rouquerol, F., Grillet, Y., and Torralvo, M. J. (1984) Influence of the orientation of the nitrogen molecule upon its actual cross-sectional area in the adsorbed monolayer: in *Fundamentals of Adsorption,* A. L. Myers and G. Belfort, eds., Engineering Foundation, New York, 501–512.

Serna, C., Rautureau, M., Prost, R., Tchoubar, C., and Serratosa, J. M. (1974) Etude de la sépiolite à l'aide des données de la microscopie électronique de l'analyse thermopondérale et de la spectroscopie infra-rouge: *Bull. Groupe Franç. Argiles* **26,** 153–163.

Serna, C., Ahlrichs, J. L., and Serratosa, J. M. (1975) Folding in sepiolite crystals: *Clays & Clay Minerals* **23,** 452–457.

Serna, C. and Van Scoyoc, G. E. (1979) Infrared study of sepiolite and palygorskite surfaces: in *Proc. Int. Clay Conf. Oxford, 1978,* M. M. Mortland and V. C. Farmer eds., Elsevier, Amsterdam, 197–206.

Sing, K. S. W. (1967) Assessment of microporosity: *Chemistry and Industry,* 829–830.

Sing, K. S. W., Everett, D. H., Haul, R. A. W., Moscou, L., Pierotti, R. A., Rouquerol, J., and Siemieniewska, T. (1985) Reporting physisorption data for gas/systems, IUPAC recommendation: *Pure Appl. Chem.* **57,** 603–619.

Van Scoyoc, G. E., Serna, C., and Ahlrichs, J. L. (1979) Structural change in palygorskite during dehydration and dehydroxylation: *Amer. Mineral.* **64,** 216–223.

Yvon, J., Baudracco, J., Cases J. M., and Weiss, J. (1990) Eléments de minéralogie quantitative en micro-analyse des argiles: in *Matériaux Argileux, Structure, Propriétés et Applications,* A. Decarreau, ed., SFMC, GFA, Paris, 473–489.

(Received 28 April 1990; accepted 30 September 1990; Ms. 2004)